
¹⁸F-Fluoromisonidazole Quantification of Hypoxia in Human Cancer Patients Using Image-Derived Blood Surrogate Tissue Reference Regions

Mark Muzi¹, Lanell M. Peterson¹, Janet N. O'Sullivan², James R. Fink¹, Joseph G. Rajendran¹, Lena J. McLaughlin¹, John P. Muzi¹, David A. Mankoff³, and Kenneth A. Krohn¹

¹Department of Radiology, University of Washington, Seattle, Washington; ²School of Mathematics, Department of Statistics, University College Cork, Cork, Ireland; and ³Department of Radiology, University of Pennsylvania, Philadelphia, Pennsylvania

¹⁸F-fluoromisonidazole (¹⁸F-FMISO) is the most widely used PET agent for imaging hypoxia, a condition associated with resistance to tumor therapy. ¹⁸F-FMISO equilibrates in normoxic tissues but is retained under hypoxic conditions because of reduction and binding to macromolecules. A simple tissue-to-blood (TB) ratio is suitable for quantifying hypoxia. A TB ratio threshold of 1.2 or greater is useful in discriminating the hypoxic volume (HV) of tissue; TB_{max} is the maximum intensity of the hypoxic region and does not invoke a threshold. Because elimination of blood sampling would simplify clinical use, we tested the validity of using imaging regions as a surrogate for blood sampling. **Methods:** Patients underwent 20-min ¹⁸F-FMISO scanning during the 90- to 140-min interval after injection with venous blood sampling. Two hundred twenty-three ¹⁸F-FMISO patient studies had detectable surrogate blood regions in the field of view. Quantitative parameters of hypoxia (TB_{max}, HV) derived from blood samples were compared with values using surrogate blood regions derived from the heart, aorta, or cerebellum. In a subset of brain cancer patients, parameters from blood samples and from the cerebellum were compared for their ability to independently predict outcome. **Results:** Vascular regions of heart showed the highest correlation to measured blood activity ($R^2 = 0.84$). For brain studies, cerebellar activity was similarly correlated to blood samples. In brain cancer patients, Kaplan–Meier analysis showed that image-derived reference regions had predictive power nearly identical to parameters derived from blood, thus obviating the need for venous sampling in these patients. **Conclusion:** Simple static analysis of ¹⁸F-FMISO PET captures both the intensity (TB_{max}) and the spatial extent (HV) of tumor hypoxia. An image-derived region to assess blood activity can be used as a surrogate for blood sampling in quantification of hypoxia.

Key Words: hypoxia; PET; ¹⁸F-FMISO; quantitation

J Nucl Med 2015; 56:1223–1228

DOI: 10.2967/jnumed.115.158717

Hypoxia imaging strategies were developed to identify an important factor that limits response to cancer treatment, because of

Received Apr. 3, 2015; revision accepted Jun. 15, 2015.
For correspondence contact: Mark Muzi, University of Washington, 1959 NE Pacific St., Seattle, WA 98195-6004.
E-mail: muzi@uw.edu
Published online Jun. 25, 2015.
COPYRIGHT © 2015 by the Society of Nuclear Medicine and Molecular Imaging, Inc.

decreased blood flow and drug delivery, decreased proliferation with fewer cycling cells, and the genomic component of HIF (hypoxia-inducing factor) signaling (1). Tumors have chronically hypoxic areas due to a mismatch between vascular supply and cellular growth. Although ionizing radiation is a strategy for killing cancer cells that does not rely on vascular delivery, the cytotoxicity of ionizing radiation depends on the O₂ level. Radiation oncologists have devised numerous strategies to overcome the therapy-limiting consequences of hypoxia but with little success (2,3). Hypoxia imaging has 2 clinically important roles: selecting a cohort of patients who might respond better to treatments designed to overcome the limitations of hypoxia and identifying the location of hypoxia in support of intensifying therapy, for example, escalating radiation dose (4–6).

Calibrated O₂-sensitive electrodes can directly measure oxygen partial pressure (PO₂, mm Hg), but the signal becomes small in hypoxia. Furthermore, electrodes are invasive, require image-guidance, and cannot access many tumors (7). Hypoxia is a phenomenologic concept with no specific concentration of tissue PO₂ that results in a transition from normoxia to hypoxia. The consequences of hypoxia occur when O₂ levels are too low to satisfy metabolic demand. Therefore, the best way to measure hypoxia would be with a biomarker that competes directly with intracellular O₂, where the agent was not trapped with sufficient O₂ but retained when O₂ supply was inadequate to accommodate mitochondrial respiration. The mechanism of ¹⁸F-fluoromisonidazole (¹⁸F-FMISO) distribution and retention meets these characteristics (1). However, any attempt to infer PO₂ from hypoxia images is misguided.

¹⁸F-FMISO is the most widely used radiotracer for assessing tissue hypoxia with PET. Its initial tissue distribution after injection is correlated to blood flow (8) because it is freely diffusible. At a PO₂ less than 3 mm Hg, nitroimidazoles such as ¹⁸F-FMISO are reduced to a product that is retained in viable hypoxic cells for the duration of the imaging study (9). Normoxic tissues equilibrate with blood after an hour (9,10). However, longer uptake times are advantageous to minimize unreduced tracer by excretion and improve image contrast. Retention of reduced ¹⁸F-FMISO by covalent binding in tissues correlates with the severity of hypoxia (11,12).

Several methods have been proposed for analyzing ¹⁸F-FMISO PET data to quantify oxygenation in human patients (13–15). Our group initially developed a kinetic model with dynamic imaging and arterial sampling, an approach validated using cancer cell spheroids in culture or in animals (16). This approach proved excessively complicated in practice and did not provide useful information because ¹⁸F-FMISO has a nearly uniform distribution in almost every tissue after 1 h (17). Our first reports quantifying ¹⁸F-FMISO

hypoxia in animal and human studies examined tissue-to-muscle and tissue-to-blood (TB) ratios to normalize uptake to a reference activity (10,18). The tissue-to-muscle values produced a variable normalization factor compromised by hypoxic muscle that was compressed during the imaging period. The use of a simple TB ratio adequately and consistently quantified tissue hypoxia. An empiric hypoxic TB threshold ratio of 1.2 or greater, developed over decades of examining thousands of normal and tumor tissues, is useful in discriminating the hypoxic volume (HV) of tissue regions (19).

The maximum TB value in the tumor region, TB_{max} , reflects the intensity of uptake, whereas the volume of pixels in a tumor that exceeds the hypoxic threshold is the HV and reflects the extent of hypoxia. Both of these parameters (TB_{max} and HV) have been shown to be independent predictors of patient outcome in brain cancer (20), head and neck cancer (H&N) (21), and sarcoma (22). However, elimination of blood sampling and analysis requiring a cross-calibrated well counter would be advantageous. The use of standardized uptake value, which is common in ^{18}F -FDG PET, would not be appropriate because it fails to account for differences in clearance of background activity. The effect on quantification of TB using reference tissue regions from ^{18}F -FMISO images as surrogates for blood sampling was evaluated. Hypoxic parameters determined from image-derived (ID) blood surrogate regions were also examined for their ability to predict survival and time-to-progression (TTP) in a brain cancer cohort (20).

MATERIALS AND METHODS

Patient Characteristics

Two hundred twenty-three ^{18}F -FMISO imaging studies on 187 cancer patients (64 glioma, 79 H&N, 14 breast, 17 sarcoma, 10 lung, 2 lymphoma, and 1 melanoma) who had 269 detectable blood surrogate regions in the imaging field of view (FOV) were recruited from the Veterans' Administration Puget Sound Health Care System, University of Washington Medical Center, and Harborview Medical Center (Table 1). Signed informed consent forms, as approved by the respective Investigational Review Boards and Radiation Safety Committees, were obtained for all patients before imaging. Early studies were done under the Radioactive Drug Research Committee, but most were performed under investigational new drug approval. Many of these patients (73 H&N, 27 glioblastoma, 11 sarcoma, and 7 breast) were included in previous reports examining survival prediction or the re-

lationship of ^{18}F -FDG to ^{18}F -FMISO imaging (20–22). A more complete description of the patients appears in the supplemental materials (available at <http://jnm.snmjournals.org>).

Radiosynthesis

^{18}F -FMISO was initially prepared using the glycidyl tosylate method (23), then changed to the method developed by Lim and Berridge (24) and modified by Adamsen et al. (25). In all cases, the same purification by high-performance liquid chromatography was used. The product specific activity ranged from 37 to 74 GBq/ μ mol at the time of injection, with greater than 98% radiochemical purity. ^{18}F -FMISO was administered by venous injection of a 10-mL solution of isotonic saline containing less than 10% (v/v) ethanol USP. The average injected dose for all studies was 267 MBq (range, 370–148 MBq).

PET Imaging

Most of the PET scans ($n = 195$) used in this analysis were performed on an Advance tomograph (GE Healthcare) operating in either 3-dimensional high-sensitivity mode at a 30-cm FOV for brain studies or 2-dimensional high-resolution mode at a 55-cm FOV for nonbrain studies. Twenty-eight studies were performed on a Discovery scanner (GE Healthcare) in 3-dimensional mode at either a 30-cm FOV for brain studies ($n = 21$) or a 55-cm FOV for body studies ($n = 7$). Emission images from both scanners were reconstructed and decay-corrected using previously described methods (26). Tomograph sensitivity was calibrated every 3 mo using a 20-cm cylindrical phantom containing a known amount of ^{18}F (Bq/mL) and processed using the same protocol as the patient studies. The well counter for determining blood activity (Cobra; Packard Instruments Inc.) was cross-calibrated at the time of scanner calibration using aliquots from the calibration phantom.

After patient immobilization, venous lines were established in each arm, one for injection and the other for blood sampling, followed by a 25-min transmission scan for the Advance or a 6-s low-dose CT scan (120 KVP, 60A) for the Discovery. A 20-min single-FOV emission scan of the tumor region was acquired during the interval of 90–140 min after injection. In 7 studies in which an adequate blood pool was not in the FOV, additional emission and transmission scans over the heart immediately preceded or followed tumor imaging. Blood samples were acquired during both scans. Typical ^{18}F -FMISO patient images of tumor uptake appear in the supplemental materials.

Blood Sampling

During emission tomography, 3 or more venous blood samples were obtained, and the activity of 1-mL aliquots was assayed in a calibrated well counter as described above. Averaged blood activity was decay-corrected to the injection time and converted to the same units as the scanner (Bq/mL).

Image Analysis

For brain studies, MR images acquired within 2 wk of the PET scan were registered with the ^{18}F -FMISO images to aid in delineating a tissue volume of interest (VOI). Conventional anatomic images (CT, MR) and PET emission scans were used with side-by-side visualization to guide VOI construction for body images. Tumor VOIs encompassing the entire tumor volume were constructed using either Alice (Parexcel) or PMOD (version 3.4; PMOD Technologies), after which they were applied to the ^{18}F -FMISO images. Tumor VOIs were 4–750 mL and did not require partial-volume correction. The ^{18}F -FMISO image data were normalized by the average blood activity to produce pixel-level TB values. HV was determined as the volume of pixels in the tumor VOI with a TB ratio of 1.2 or greater, indicating significant hypoxia (21). For each tumor, the pixel with the maximum TB value (TB_{max}) and HV were determined.

Quantification of ^{18}F -FMISO in ID tissue regions used as surrogates for blood activity were performed as follows: for heart, 3-cm circular

TABLE 1
 ^{18}F -FMISO Patient Region Summary

Cancer type	ID blood regions		
	Cerebellum	Aorta	Heart
Brain	93		
H&N	75	4	3
Sarcoma	2	21	17
Breast		15	15
Lung		10	8
Lymphoma		2	2
Melanoma		1	1
Total regions	170	53	46

Two hundred twenty-three studies on 187 patients were selected on the basis of presence of detectable surrogate normoxic tissue.

regions were placed on approximately 2 cm of axial distance over the left ventricular cavity; for aorta, 1-cm circular regions were placed on approximately 3 cm of axial distance; and for cerebellum, two 2-cm-diameter regions were placed on the left and right cerebellar cortex over approximately 1 cm of axial distance (Fig. 1). Although brain regions are generally normoxic, the cerebellum was selected because brain tumors in adults are typically supratentorial and may undergo severe morphologic deformation during disease progression (27), preventing the selection of consistent areas of normoxic brain without infiltrative glioma cells. Additionally, H&N cancer patients often have cerebellum in the FOV, so this region is adequate for both cancers. Several imaging studies had multiple surrogate blood regions, such as cardiac and aortic regions in lung and breast cancer studies. The total number of regions assessed was 269 (170 cerebellum, 46 heart, 53 aorta) from 223 studies on 187 patients.

Statistical Analysis

Correlation and regression statistics for comparison of ID tissue and sampled blood activity with their associated hypoxia parameters were performed using JMP (SAS Institute). The comparison of the hypoxia parameters TB_{max} and HV determined from ID and blood sampling was assessed using regression and Bland–Altman plots to investigate statistical agreement.

To assess ID hypoxia parameters as independent predictors of outcome, we used a cohort of glioma patients imaged before conventional therapy. Our previous report (20), which included 22 glioma patients, relied on blood samples for the determination TB_{max} and HV and showed predictive value for outcomes. For the current study, the original cohort of patients was expanded to 38 patients.

Univariate and multivariate Cox proportional hazards regression analysis (28) were used to compare the capability of hypoxic parameters determined from both measured and ID blood to predict TTP and survival. Progression was defined by the response assessment in

neuro-oncology criteria (RANO) for glioma patients (29). Analyses were considered for overall survival and survival at 2 y, the median survival for patients diagnosed with primary brain cancer (30). Cox multivariate analysis used the hypoxia parameters along with the following conventional predictors: extent of resection, age, sex, and Karnofsky performance score. Grade was not included as 34 of the 38 glioma patients were World Health Organization grade 4. All continuous variables were standardized, so that the hazard ratio represents an increase in risk associated with an SD increase for the variable. Survival analyses were performed in R (R Development Core 2014).

RESULTS

Average parameters for blood reference tissue regions, along with the blood surrogate hypoxia parameters, are presented in Table 2. Overall, surrogate blood regions showed a high correlation ($R^2 = 0.84$, $n = 269$) to measured blood (Table 3). For studies with cerebellum in the FOV, ID blood activity was highly correlated to sampled blood ($R^2 = 0.84$, $n = 170$). Other surrogate regions showed a similar relationship to measured blood (heart $R^2 = 0.84$, $n = 46$; aorta $R^2 = 0.83$, $n = 53$).

The injected dose had a low correlation ($R^2 = 0.42$) to blood activity (Fig. 2A). Bland–Altman plots (Fig. 2B) for blood activity (MBq/mL) and normalized dose (MBq/kg) showed a severe bias and structure. The regression of ID TB_{max} versus TB_{max} showed values clustered around the line of identity (slope = 0.98, intercept = 0.04, SEE/mean = 7% error) and was similar for HV. Bland–Altman plots of TB_{max} and HV with their coordinate ID parameters all showed little bias, with clustering within the SE limits of ± 2 SDs (Fig. 3). Examination of sampled blood and ID blood data using Bland–Altman plots for individual ID regions showed agreement between measures. The data were clustered around the mean and showed little bias or structure. The average percentage difference between blood and ID values also showed minimal bias (TB_{max} , 1.3%; HV, 6.9%). Overall, the relationship between measured blood and ID blood was consistent (tables and figures in the supplemental material).

Kaplan–Meier survival curves are given for both survival and TTP for TB_{max} and ID TB_{max} variables for 2 y (Fig. 4). Patients were classified as low or high risk by considering whether they were below or above the median TB_{max} . When overlaid on those plots, the ID TB_{max} variable shows a high degree of similarity to blood-derived TB_{max} . Overall, the ID parameters were as predictive as and showed plot characteristics similar to parameters determined using sampled blood.

Univariate analysis (Tables 4 and 5) showed that ID hypoxia parameters were as predictive as parameters determined using blood samples. Age and Karnofsky score were significantly associated with survival and TTP. Clinical information (age, sex, Karnofsky score, and resection status) was considered in multivariate models with each of the hypoxia variables (Tables 4 and 5). Multivariate Cox proportional hazards analysis showed that all measures of hypoxia (HV, ID HV, TB_{max} , ID TB_{max}) were highly significant predictors of outcomes, when the model was adjusted for clinical parameters. Hazard ratios and P values for the ^{18}F -FMISO variables and the clinical covariates all remained similar when the ID variables replaced the ones using sampled blood. R^2 values for the models were also similar, with the greatest absolute change being 2% for the comparison of TTP using TB_{max} or ID TB_{max} ($R^2 = 0.47$ for the TB_{max} model versus $R^2 = 0.49$ for the ID TB_{max} model). Age was the only variable that added prognostic utility when included with hypoxia information using a backward-elimination approach (not shown).

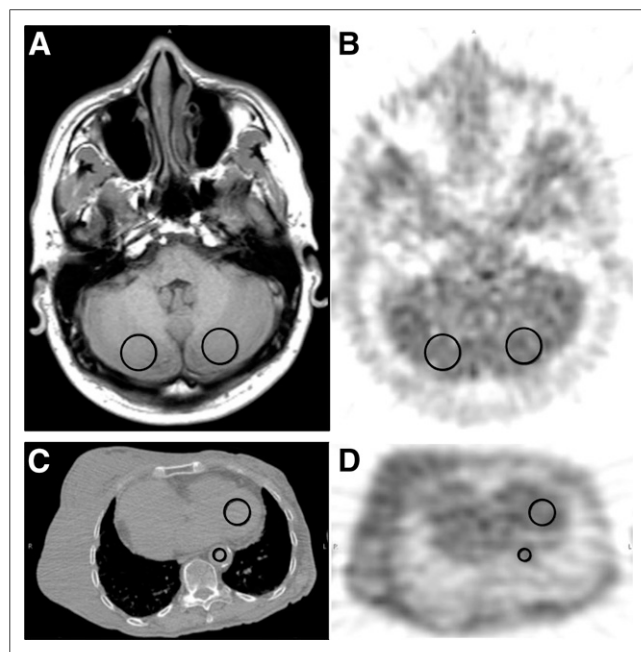


FIGURE 1. ^{18}F -FMISO image analysis. MR image (A) registered to a PET ^{18}F -FMISO image (B) showing placement of 2-cm-diameter cerebellar regions of interest to determine surrogate blood activity. Example of cardiac (3-cm diameter) and aortic region of interest (1-cm diameter) on low-dose CT scan used for attenuation correction (C) and PET ^{18}F -FMISO scan (D). Patient examples of ^{18}F -FMISO tumor uptake appear in supplemental materials.

TABLE 2
Blood and Hypoxia Parameter Mean Values

Parameter	Cerebellum (170*)	Aorta (53*)	Heart (46*)
Blood [†]	1.51 ± 0.22	1.46 ± 0.24	1.45 ± 0.25
ID blood [†]	1.50 ± 0.21	1.42 ± 0.23	1.45 ± 0.25
TB _{max}	1.77 ± 0.55	1.72 ± 0.68	1.74 ± 0.70
ID TB _{max}	1.77 ± 0.56	1.78 ± 0.72	1.77 ± 0.78
HV (mL)	20.6 ± 38.5	35.1 ± 57.0	34.5 ± 53.5
ID HV (mL)	20.9 ± 42.2	35.4 ± 56.0	35.7 ± 55.3

*No. of regions analyzed for each blood surrogate.

[†]Values for blood and ID blood are SUV.

Values presented are mean ± SD. Blood, TB_{max}, and HV values were derived from blood sampling. ID blood, ID TB_{max}, and ID HV were determined from blood reference tissue regions.

Karnofsky score and sex did not add information to the model. HV survival results appear in the supplemental materials.

DISCUSSION

Since the introduction of the kinetic model of ¹⁸F-FMISO metabolism to estimate hypoxia in tumor spheroids (16), work on alternative, simpler methods to assess ¹⁸F-FMISO retention and reduce blood sampling and imaging time have been reported (5,14,15,31). These techniques have shortcomings associated with the measurement and interpretation. The complexity of dynamic imaging with arterial sampling is unwarranted for a tracer that distributes in tissue by a partition coefficient mechanism. Agents with partition coefficients far from unity may warrant a more complicated dynamic analysis to separate delivery from retention (32,33). A stable reference such as blood is preferred to normalize ¹⁸F-FMISO uptake to tracer delivery by computing a tissue-to-blood partition coefficient (34). The TB ratio provides a reliable and consistent measure of HV, which is based on the retention of reduced ¹⁸F-FMISO under conditions of low PO₂.

The impact of using an ID tissue surrogate for blood in determining ID HV in glioma patients produced an average bias of approximately 6% and was considered minimal. The average bias for cardiac and aortic surrogates for ID HV in nonneural tumors was 4% and 8%, respectively. This is tolerable as a trade-off to eliminate blood sampling from the protocol.

Imaging ¹⁸F-FMISO in several cancer types, with identification of vasculature through coordinate CT or MR mapping, provides an

ID surrogate that is directly correlated to sampled blood activity. Studies that imaged the heart separately from tumor illustrate that a region without a blood pool can be used to quantify ¹⁸F-FMISO, provided that a secondary scan over the heart can be acquired. Results from ¹⁸F-FMISO brain studies show a high correlation between cerebellar and venous blood activity. These correlative results suggest that quantifying ¹⁸F-FMISO hypoxia parameters can be based on ID surrogate activity that has been shown to correlate to sampled blood.

An alternative analysis without blood sampling could be considered based on the relationship between the weight-normalized injected dose and sampled blood activity. The normalized injected dose (MBq/kg) showed poor correlation ($R^2 = 0.42$, $n = 223$) to

TABLE 3
Correlation of Blood to ID Blood Surrogates

Blood surrogate	<i>n</i>	R^2	Slope	ρ	SEE/mean
Cerebellum	170	0.84	0.89	0.92	0.06
Heart	46	0.84	0.92	0.92	0.07
Aorta	53	0.83	0.87	0.91	0.07
Overall	269	0.84	0.89	0.91	0.06

Correlation results of ID to sampled blood activity. Correlation parameters are R^2 (coefficient of determination), slope from linear regression, Pearson ρ , and SEE/mean as a measure of coefficient of variation of regression.

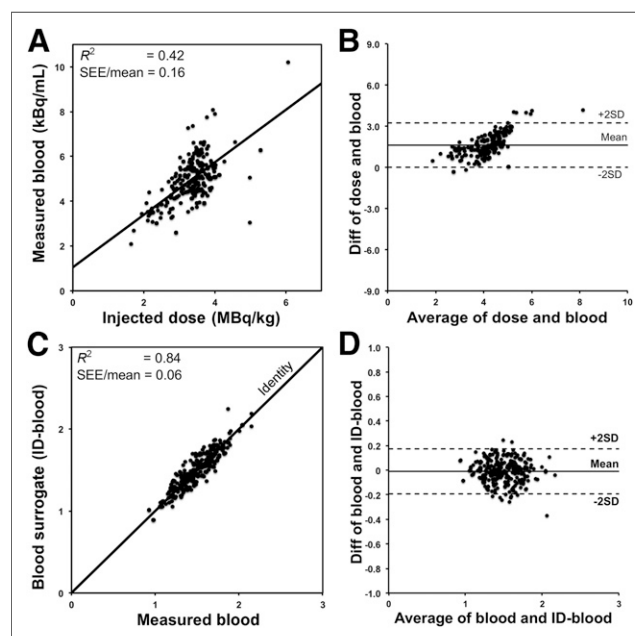


FIGURE 2. Correlation of blood and ID blood. (A) Normalized injected dose (MBq/kg) showed poor correlation ($R^2 = 0.42$, $n = 223$) to measured blood activity (kBq/mL). (B) Bland–Altman plot of data shows unusual structure with points generally lying obliquely to mean, indicating poor linear relationship. Regression (C) and Bland–Altman (D) plots between measured blood and surrogate blood regions (ID blood) showed high correlation at $R^2 = 0.84$.

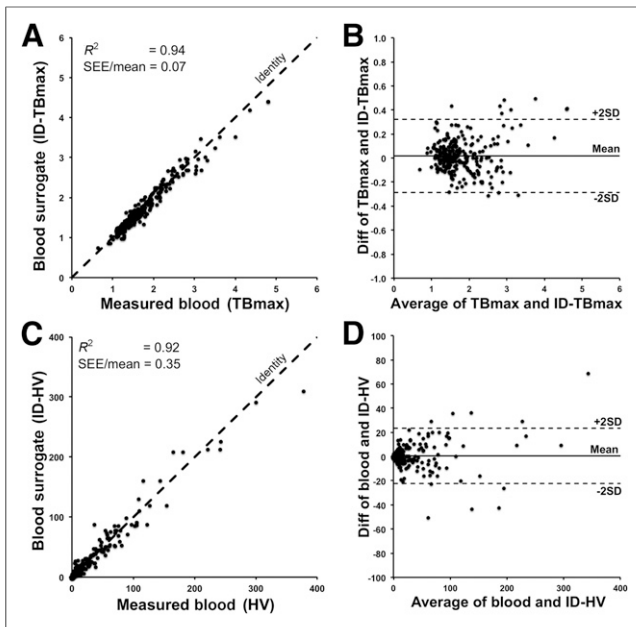


FIGURE 3. Correlation of hypoxia parameters. (A) Regression plot of TB_{max} vs. ID TB_{max} for 269 surrogate blood regions shows strong relationship with small coefficient of variation (SEE/mean). (B) Bland–Altman plot shows clustering around mean with little bias. Plots of HV vs. ID HV values in C and D show similar profile.

blood activity concentration (Bq/mL), and the Bland–Altman plot of the data shows structure with points generally lying obliquely to the mean, indicating a poor linear relationship. We conclude that normalizing to injected dose is not valid.

Previously, we reported on the predictive value of TB_{max} and HV determined from blood samples for outcome in glioma patients (20). Survival analysis using ^{18}F -FMISO imaging results from 38 brain tumor patients support the hypothesis that a greater hypoxic tumor burden before therapy predicts shorter survival and TTP. However, these results imply that more HV means more tumor is at risk for the genomic consequences of hypoxia. This interpretation may apply to HV, but the tumor

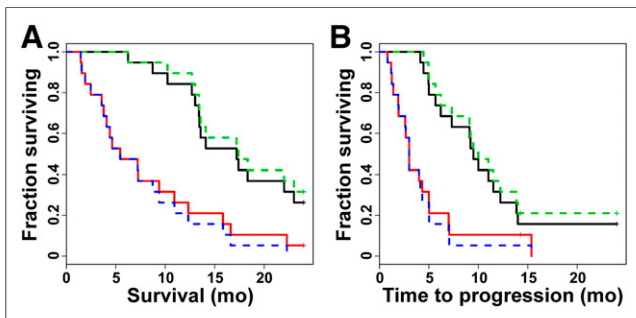


FIGURE 4. Kaplan–Meier survival analysis. Hypoxia parameters were used to stratify 38 pretreatment glioma patients with respect to 2-y survival and TTP. Kaplan–Meier plots for TB_{max} demonstrated significantly shorter survival (A) and TTP (B) in high-risk patients (red line) whose tumors possessed TB_{max} ratios greater than median ($TB_{max} > 1.83$) relative to low-risk patients (black line). Using cerebellum as blood surrogate produced hypoxia parameter ID TB_{max} (dotted lines, median ID $TB_{max} = 1.77$) that had nearly predictive power nearly identical to TB_{max} . Kaplan–Meier plots and results for HV appear in supplemental materials.

TABLE 4
Results of Univariate Analysis for Predictors of Outcome in Pretreatment Glioma Patients ($n = 38$)

Predictor	Survival		TTP	
	Hazard	<i>P</i>	Hazard	<i>P</i>
Age	1.73	0.005	1.73	0.004
Sex	1.77	0.144	1.80	0.131
KPS*	0.63	0.019	0.67	0.028
HV	2.30	<0.001	2.07	<0.001
ID HV	2.69	<0.001	2.45	<0.001
TB_{max}	2.51	<0.001	2.34	<0.001
ID TB_{max}	2.41	<0.001	2.31	<0.001
Resection†	1.21	0.604	1.16	0.664

*Karnofsky performance score.

†Resection is dichotomized as biopsy or other (gross/subtotal resection).

Univariate analysis of hypoxia and clinical variables shows the hazard ratio with *P* values associated with the outcome variables survival and TTP at 2 y.

TB_{max} or ID TB_{max} as indicators of hypoxia are less dependent on tumor volume. TB_{max} has the advantage of not requiring an empiric

TABLE 5
Results of Multivariate Cox Regression Analysis for Predictors of Outcome in Pretreatment Glioma Patients ($n = 38$)

Predictor	Survival (0.390)*		TTP (0.466)	
	Hazard	<i>P</i>	Hazard	<i>P</i>
Age	1.26	0.421	1.44	0.158
Sex	1.77	0.525	1.43	0.440
KPS†	0.78	0.324	0.88	0.554
TB_{max}	2.37	<0.001	2.31	<0.001
Resection‡	0.76	0.516	0.75	0.463

Predictor	Survival (0.394)		TTP (0.485)	
	Hazard	<i>P</i>	Hazard	<i>P</i>
Age	1.22	0.483	1.38	0.210
Sex	1.23	0.676	1.31	0.559
KPS	0.75	0.244	0.82	0.378
ID TB_{max}	2.30	<0.001	2.30	<0.001
Resection	0.81	0.616	0.77	0.519

*The coefficient of determination (R^2) is given for each table.

†Karnofsky performance score.

‡Resection is dichotomized as biopsy or other (gross/subtotal resection).

Multivariate analysis shows that after adjusting for clinical variables using a multivariate Cox model, greater tumor TB_{max} was still associated with shorter survival and TTP. Multivariate results for HV and ID HV appear in supplemental materials.

threshold for hypoxia assessment, and ID TB_{max} has a further advantage of not requiring blood sampling. Survival analyses of hypoxic parameters determined without blood sampling were nearly identical to those determined with blood samples. This suggests that the most parsimonious method for quantifying hypoxia with ^{18}F -FMISO is an imaging session after partition equilibrium with no blood sampling to yield hypoxic parameters useful for assessing response and predicting outcome.

CONCLUSION

ID tissue regions that are highly correlated to blood levels can be used as surrogates in the quantification of hypoxia parameters for ^{18}F -FMISO imaging (TB_{max} and HV). This association supports the elimination of serial blood sampling during ^{18}F -FMISO imaging. Reducing the complexity of ^{18}F -FMISO imaging through a short static imaging session without blood sampling is a parsimonious method to delineate tumor hypoxia without compromising the efficacy of the hypoxic assessment, which makes it suitable as a routine clinical procedure and for large clinical trials.

DISCLOSURE

The costs of publication of this article were defrayed in part by the payment of page charges. Therefore, and solely to indicate this fact, this article is hereby marked "advertisement" in accordance with 18 USC section 1734. Our research was supported by the National Cancer Institute (P01-CA042045, R01-CA72064), a NIH major equipment grant (RR-017229), ACRIN (U01CA079778 and U01CA080098), and the Science Foundation of Ireland (11/PI/1027). No other potential conflict of interest relevant to this article was reported.

ACKNOWLEDGMENTS

Our initial studies of hypoxia were motivated by Drs. Janet Rasey, Wui-Jin Koh, Janet Eary, and Alexander Spence, who we gratefully acknowledge for their contribution toward our perspective on hypoxia imaging. We also acknowledge the effort of Dr. Jeanne Link and the UW radiochemistry group for the many productions of ^{18}F -FMISO.

REFERENCES

- Rajendran JG, Krohn KA. F-18 fluoromisonidazole for imaging tumor hypoxia: imaging the microenvironment for personalized cancer therapy. *Semin Nucl Med.* 2015;45:151–162.
- Overgaard J. Hypoxic radiosensitization: adored and ignored. *J Clin Oncol.* 2007;25:4066–4074.
- Degner FL, Sutherland RM. Mathematical modelling of oxygen supply and oxygenation in tumor tissues: prognostic, therapeutic, and experimental implications. *Int J Radiat Oncol Biol Phys.* 1988;15:391–397.
- Lee NY, Mechalakos JG, Nehmeh S, et al. Fluorine-18-labeled fluoromisonidazole positron emission and computed tomography-guided intensity-modulated radiotherapy for head and neck cancer: a feasibility study. *Int J Radiat Oncol Biol Phys.* 2008;70:2–13.
- Thorwarth D, Eschmann SM, Paulsen F, Alber M. A model of reoxygenation dynamics of head-and-neck tumors based on serial ^{18}F -fluoromisonidazole positron emission tomography investigations. *Int J Radiat Oncol Biol Phys.* 2007;68:515–521. Epub 2007 Mar 2029.
- Hendrickson K, Phillips M, Smith W, Peterson L, Krohn K, Rajendran J. Hypoxia imaging with [F-18] FMISO-PET in head and neck cancer: potential for guiding intensity modulated radiation therapy in overcoming hypoxia-induced treatment resistance. *Radiother Oncol.* 2011;101:369–375.
- Bartlett RM, Beattie BJ, Naryanan M, et al. Image-guided PO2 probe measurements correlated with parametric images derived from ^{18}F -fluoromisonidazole small-animal PET data in rats. *J Nucl Med.* 2012;53:1608–1615.

- Martin GV, Caldwell JH, Rasey JS, Grunbaum Z, Cerqueira M, Krohn KA. Enhanced binding of the hypoxic cell marker [3H]fluoromisonidazole in ischemic myocardium. *J Nucl Med.* 1989;30:194–201.
- Rasey JS, Casciari JJ, Hofstrand PD, Muzi M, Graham MM, Chin LK. Determining hypoxic fraction in a rat glioma by uptake of radiolabeled fluoromisonidazole. *Radiat Res.* 2000;153:84–92.
- Rasey JS, Grunbaum Z, Magee S, et al. Characterization of radiolabeled fluoromisonidazole as a probe for hypoxic cells. *Radiat Res.* 1987;111:292–304.
- Rasey JS, Nelson NJ, Chin L, Evans ML, Grunbaum Z. Characteristics of the binding of labeled fluoromisonidazole in cells in vitro. *Radiat Res.* 1990;122:301–308.
- Gross MW, Karbach U, Groebe K, Franko AJ, Mueller-Klieser W. Calibration of misonidazole labeling by simultaneous measurement of oxygen tension and labeling density in multicellular spheroids. *Int J Cancer.* 1995;61:567–573.
- Thorwarth D, Eschmann SM, Paulsen F, Alber M. A kinetic model for dynamic [^{18}F]Fmiso PET data to analyse tumour hypoxia. *Phys Med Biol.* 2005;50:2209–2224.
- Eschmann SM, Paulsen F, Bedeshem C, et al. Hypoxia-imaging with ^{18}F -misonidazole and PET: changes of kinetics during radiotherapy of head-and-neck cancer. *Radiother Oncol.* 2007;83:406–410.
- Wang W, Georgi JC, Nehmeh SA, et al. Evaluation of a compartmental model for estimating tumor hypoxia via FMISO dynamic PET imaging. *Phys Med Biol.* 2009;54:3083–3099.
- Casciari JJ, Chin LK, Livesey JC, Boyles D, Steen RG, Rasey JS. Growth rate, labeling index, and radiation survival of cells grown in the Matrigel thread in vitro tumor model. *In Vitro Cell Dev Biol Anim.* 1995;31:582–589.
- Grunbaum Z, Freauff SJ, Krohn KA, Wilbur DS, Magee S, Rasey JS. Synthesis and characterization of congeners of misonidazole for imaging hypoxia. *J Nucl Med.* 1987;28:68–75.
- Rasey JS, Koh WJ, Grierson JR, Grunbaum Z, Krohn KA. Radiolabelled fluoromisonidazole as an imaging agent for tumor hypoxia. *Int J Radiat Oncol Biol Phys.* 1989;17:985–991.
- Rajendran JG, Krohn KA. Imaging tumor hypoxia. In: Valk PE, Bailey DL, Townsend DW, Maisey MN, eds. *Positron Emission Tomography, Principles and Practice.* London, U.K.: Springer Verlag; 2002:689–695.
- Spence AM, Muzi M, Swanson KR, et al. Regional hypoxia in glioblastoma multiforme quantified with [^{18}F]fluoromisonidazole positron emission tomography before radiotherapy: correlation with time to progression and survival. *Clin Cancer Res.* 2008;14:2623–2630.
- Rajendran JG, Schwartz DL, O'Sullivan J, et al. Tumor hypoxia imaging with [F-18] fluoromisonidazole positron emission tomography in head and neck cancer. *Clin Cancer Res.* 2006;12:5435–5441.
- Rajendran JG, Wilson DC, Conrad EU, et al. [^{18}F]FMISO and [^{18}F]FDG PET imaging in soft tissue sarcomas: correlation of hypoxia, metabolism and VEGF expression. *Eur J Nucl Med Mol Imaging.* 2003;30:695–704.
- Grierson JR, Link JM, Mathis CA, Rasey JS, Krohn KA. A radiosynthesis of fluorine-18 fluoromisonidazole. *J Nucl Med.* 1989;30:343–350.
- Lim JL, Berridge MS. An efficient radiosynthesis of [^{18}F]fluoromisonidazole. *Appl Radiat Isot.* 1993;44:1085–1091.
- Adamsen TCH, Grierson JR, Krohn KA. A new synthesis of the labeling precursor for F-18 -fluoromisonidazole. *J Labelled Comp Radiopharm.* 2005;48:923–927.
- Lewellen TK, Kohlmyer SG, Miyaoka RS, Kaplan MS, Stearns CW, Schubert SF. Investigation of the performance of the general electric ADVANCE positron emission tomograph in 3D mode. *IEEE Trans Nucl Sci.* 1996;43:2199–2206.
- Chintagumpala M, Gajjar A. Brain tumors. *Pediatr Clin North Am.* 2015;62:167–178.
- Cox DR, Oakes D. *Analysis of Survival Data.* Boca Raton, FL: Chapman & Hall; 1984.
- Wen PY, Macdonald DR, Reardon DA, et al. Updated response assessment criteria for high-grade gliomas: response assessment in neuro-oncology working group. *J Clin Oncol.* 2010;28:1963–1972.
- Van Meir EG, Hadjipanayis CG, Norden AD, Shu HK, Wen PY, Olson JJ. Exciting new advances in neuro-oncology: the avenue to a cure for malignant glioma. *CA Cancer J Clin.* 2010;60:166–193.
- Bruehlmeier M, Roelcke U, Schubiger PA, Ametamey SM. Assessment of hypoxia and perfusion in human brain tumors using PET with ^{18}F -fluoromisonidazole and ^{15}O -H $_2$ O. *J Nucl Med.* 2004;45:1851–1859.
- Shi K, Souvatzoglou M, Astner ST, et al. Quantitative assessment of hypoxia kinetic models by a cross-study of dynamic ^{18}F -FAZA and ^{15}O -H $_2$ O in patients with head and neck tumors. *J Nucl Med.* 2010;51:1386–1394.
- Verwer EE, van Velden FH, Bahce I, et al. Pharmacokinetic analysis of [^{18}F]FAZA in non-small cell lung cancer patients. *Eur J Nucl Med Mol Imaging.* 2013;40:1523–1531.
- Koh WJ, Rasey JS, Evans ML, et al. Imaging of hypoxia in human tumors with [F-18]fluoromisonidazole. *Int J Radiat Oncol Biol Phys.* 1992;22:199–212.